IEEE Access
Multidisciplinary ⋮ Rapid Review ⋮ Open Access Journal

Received 1 March 2023, accepted 25 April 2023, date of publication 1 May 2023, date of current version 8 May 2023.

Digital Object Identifier 10.1109/ACCESS.2023.3271863

RESEARCH ARTICLE

Design of Higher-Order Fractional Filters With Fully Controllable Frequency Characteristics

JULIA NAKO[1], (Graduate Student Member, IEEE), COSTAS PSYCHALINOS[1], (Senior Member, IEEE), AHMED S. ELWAKIL[2,3,4], (Senior Member, IEEE), AND DRAZEN JURISIC[5], (Member, IEEE)

[1]Department of Physics, Electronics Laboratory, University of Patras, 26504 Patras, Greece
[2]Department of Electrical and Computer Engineering, University of Sharjah, Sharjah, United Arab Emirates
[3]Department of Electrical and Software Engineering, University of Calgary, Calgary, AB T2N 1N4, Canada
[4]Nanoelectronics Integrated Systems Center (NISC), Nile University, Giza 3247010, Egypt
[5]Faculty of Electrical Engineering and Computing, University of Zagreb, 10000 Zagreb, Croatia

Corresponding author: Costas Psychalinos (cpsychal@upatras.gr)

ABSTRACT Higher-order fractional filters with fully controllable frequency characteristics are realized in this work, after fitting the filter's magnitude response data using a minimum-phase state-space model. Subsequently, rational integer-order transfer functions are derived and implemented using as active elements: a) Operational Transconductance Amplifiers (OTAs) and b) a Field Programmable Analog Array (FPAA) device. The realized filters enjoy electronic adjustability of their type, order, and characteristic frequencies while being easily validated on the digitally programmable FPAA platform.

INDEX TERMS Fractional-order filters, approximation techniques, Butterworth filters, Chebyshev filters, operational transconductance amplifiers, field programmable analog arrays.

I. INTRODUCTION

Fractional-order filtering is an attractive technique for performing fine adjustment of the slope of the transition from the pass-band to the stop-band of the filter, as well as for performing scaling of the corresponding time-constants [1]. The former feature originates from the fact that the slope is expressed by the formula $\pm 20(n+\alpha)$ dB/dec., with n being the integer part of the order and $0 < \alpha < 1$ being its non-integer part. The latter feature is the result of the dependence of the filter's cutoff frequency on both the pole frequency and the order.

In the literature, fractional-order filters of orders in the range]0,1[have been developed through the following ways:

1) on the circuit level by substitution of capacitors in the conventional integer-order filters with RC networks (e.g. Foster or Cauer types) approximating the behavior of the required fractional-order capacitors [2], or
2) on the system level by employing suitable approximation tools (e.g. Oustaloup, continued fraction expansion, etc.) for approximating the Laplacian operator $s^{\alpha} = (j\omega)^{\alpha}$, used for the transposition of the integer-order transfer functions to the fractional-order domain.

The first procedure is straightforward, in the sense that the derivation of the circuitry is a one-step procedure and the calculation of the passive element values can be easily performed via a systematic way [3]. The second one is slightly more complicated, because additional algebraic operations are required for deriving the rational integer-order transfer function. On the other hand, it offers design flexibility because the designer can freely choose between multiple filter design and implementation techniques [4].

The aforementioned procedures have been also followed in the case of fractional filters of orders between one and two but without full control of the frequency characteristics of these filters. More specifically, while the slope of the pass-band and stop-band gradients are fully determined by the order of the filter, being equal to $\pm 20(1+\alpha)$ dB/dec., the

The associate editor coordinating the review of this manuscript and approving it for publication was Venkata Rajesh Pamula.

cutoff frequency is not controlled without the application of an appropriate optimization algorithm. Significant research effort has been performed to overcome this obstacle, where appropriate cost functions, error minimization, metaheuristic, and genetic algorithms have been utilized [5], [6], [7], [8], [9], [10], [11], [12], [13], [14], [15], [16], [17], [18], [19], [20], [21], [22], [23], [24]. The design of fractional-order filters with orders greater than two has been introduced in [5], [6], [7], [22], [25], [26], [27], where the aforementioned algorithms have been employed. The corresponding realizations are actually active-RC implementations of the derived rational integer-order functions and, therefore, they do not offer fully adjustable frequency characteristics of the filter structures.

In the present work, a procedure for deriving the approximation transfer functions, which realize the pre-determined frequency characteristics of the fractional-order prototype filters of order greater than two, is introduced. It is based on the fit of the frequency response magnitude data by a minimum-phase state-space model, using Log-Chebyshev magnitude design. This means that all well-known filters types, such as Butterworth and Chebyshev, can be implemented in any standard form (e.g. low-pass, high-pass or band-pass). Here, the implementation of the resulting transfer functions is performed in two different ways: (i) using Operational Transconductance Amplifiers (OTAs) as active elements, and (ii) using a Field Programmable Analog Array (FPAA) device. In both cases, full controllability of the frequency characteristics is achieved without altering the core structure that implements the integer-order approximation functions, hence offering design flexibility and versatility. The paper is organized as follows: detailed overview of the relevant literature is performed in Section II, while the proposed procedure is also introduced. Possible implementations are demonstrated in Section III, and their behavior is evaluated through simulation and experimental results in Section IV.

II. PROPOSED PROCEDURE FOR DESIGNING FRACTIONAL FILTERS OF ORDER GREATER THAN TWO

A. BACKGROUND

The expression of the magnitude response of a Butterworth low-pass transfer function of order $(n+\alpha)$, with $n \in \mathbb{N}$ and $0 < \alpha < 1$, is given by

$$\left|H_{LP,n+\alpha}(\omega)\right| = \frac{1}{\sqrt{1+\left(\frac{\omega}{\omega_0}\right)^{2(n+\alpha)}}}, \tag{1}$$

where the maximum gain is equal to one, and the half-power frequency (or equivalently the -3 dB cutoff frequency) is equal to ω_0. The first attempt for implementing fractional-order Butterworth filters of order $(n+\alpha) > 2$ was reported in [5], [6], where the (approximated) transfer function of order $(1+\alpha)$ Butterworth low-pass filter is divided by an $(n-1)$ order Butterworth polynomial, in order to realize an $(n+\alpha)$ order filter. The work in [22] introduces a new technique to optimally design the fractional-order Butterworth low-pass filters in the complex F-plane using the constrained composite differential evolution (C^2oDE) algorithm. The presented 1.5 order fractional low-pass filter realization is performed by substituting the capacitors in the well-known Sallen-Key circuit by fractional-order ones, approximated by the Valsa network [28]. The work in [25] describes the design of analog pseudo-differential fractional Butterworth filters of the order $(2+\alpha)$ operating in a mixed-transadmittance mode (voltage input, current output) and was implemented using second generation Current Conveyors (CCIIs), Differential Difference Current Conveyors (DDCCs) or Differential Voltage Current Conveyors (DVCCs) as active elements. The procedure followed was: (i) a $(2+\alpha)$ order transfer function was considered and its coefficients were determined as a function of the order of the filter using a numerical optimization algorithm to minimize the error between magnitude in dB of the considered transfer function and that in (1). For this purpose, the MATLAB function *fminsearch* with a suitable fitness function was used. (ii) The approximation of the fractional-order capacitors was performed through the utilization of Foster type-II RC networks. This work was further extended in [26], where transfer functions of low-pass/high-pass filters with Butterworth maximally flat magnitude and fractional-orders higher than two were realized. The implementation presented in [26] was based on the employment of OTAs as active elements, and the required fractional-order capacitors were approximated using the Valsa network.

The magnitude frequency response of a $(n+\alpha)$ order Chebyshev low-pass filter is given by

$$\left|H_{LP,n+\alpha}(\omega)\right| = \frac{1}{\sqrt{1+\varepsilon^2 C^2_{n+\alpha}(\omega)}}, \tag{2}$$

with $0 < \varepsilon \leq 1$ being the ripple factor, $C_{n+\alpha}(\omega) = \cos\left[(n+\alpha)\cdot\cos^{-1}\left(\frac{\omega}{\omega_0}\right)\right]$ being the corresponding Chebyshev polynomial, and ω_0 being the cutoff frequency where the gain becomes equal to $1/\sqrt{1+\varepsilon^2}$. A design procedure for realizing Chebyshev low-pass filters of order $(n+\alpha)$ was introduced in [7] where the MATLAB *lsqcurvefit* function was used to implement the non-linear least squares optimization. No implementation of a filter with order greater than two was presented in [7]. In the work of [29], metaheuristic evolutionary algorithms were employed for approximating the response of $(n+\alpha)$ order Chebyshev low-pass filters. Operational amplifier (op-amp) and OTA based implementations of orders in the range]1, 2[were reported in this work. Finally, in [27] a genetic algorithm was also employed to optimize the parameters of the fractional-order transfer function so that its magnitude characteristics approximate the ideal response of the fractional-order Chebyshev low-pass filter. It provided a design of 2.2 order low-pass filter realized using op-amps, while the Foster type-I RC network was employed for approximating the behavior of the fractional-order capacitors.

B. FREQUENCY RESPONSE MAGNITUDE APPROXIMATION

1) LOW-PASS FILTER FUNCTIONS

The gain responses described by (1)–(2) can be approximated through the following steps:

- Collect the frequency response data of (1) or (2), within the frequency range of interest, using the MATLAB *frd* function of the *Control System Toolbox*.
- Assuming an approximation order (N), obtain the rational integer-order transfer function of the filter using the MATLAB commands *fitmagfrd,* which performs the fit of the frequency response magnitude data by a minimum-phase state-space model, and *tf*, which converts the model into a transfer function. Both commands are included in the *Robust Control Toolbox.*

These steps are summarized in the following program listing, where a Butterworth low-pass filter of order equal to 2.4 is approximated. It must be mentioned at this point that only the line describing the variable *mag_ideal* of the provided code must be changed for obtaining different types of filter functions.

```
clc;
s=tf('s');
%% user data
% order of the filter
n=2;
alpha=0.4;
% characteristic frequency of the filter
wo=1;
% approximation order
approx_order=4;
% determination of the limits
w_min=wo*1E-1;
w_max=wo*1E+1;
w=logspace(log10(w_min),log10(w_max)
    ,200);
%% frequency response data
% Butterworth low-pass filter
mag_ideal=sqrt(1./(1+(w/wo).^(2*(n+alpha
    ))));

%%  curve fitting approximation
% obtaining the frequency response
    magnitude data
mag_ideal_data=frd(mag_ideal,w);
% fit of frequency response magnitude
    data
G = fitmagfrd(mag_ideal_data,
    approx_order);
% obtaining the rational integer-order
    transfer function
H_approx=minreal(tf(G))
```

Listing 1. MATLAB code for approximating a Butterworth low-pass filter.

The resulting transfer function will have the form of (3)

$$H(s) = \frac{B_N s^N + B_{N-1} s^{N-1} + \ldots + B_1 s + B_0}{s^N + A_{N-1} s^{N-1} + \ldots + A_1 s + A_0}, \quad (3)$$

with A_i and B_j ($i = 0, 1 \ldots N-1,\ j = 0, 1 \ldots N$) being positive and real coefficients. For demonstration purposes, let us consider Butterworth low-pass filter functions with cutoff frequency $\omega_0 = 1$ rad/s, which will be approximated in the frequency range $[10^{-1},\ 10^{1}]$ rad/s. Employing a 4^{th}–order approximation, the resulting values of the coefficients A_i and B_j are summarized in Table 1. The corresponding values for approximating Chebyshev low-pass filter functions, with a 3 dB ripple and the same ω_0, under the same conditions of approximation are provided in Table 2. The resulting frequency responses are depicted in Figs. 1 and 2, respectively, where the validity of the presented concept is verified.

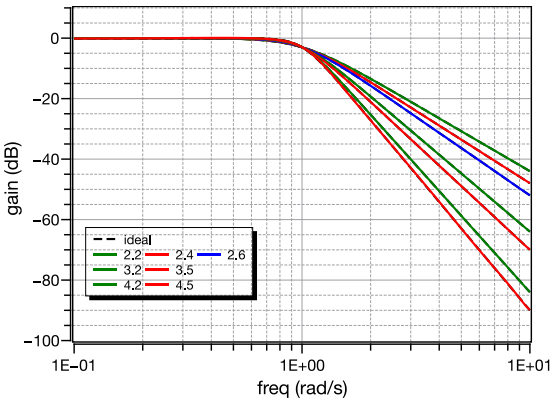

FIGURE 1. Frequency responses of the approximated Butterworth low-pass filters with the ideal responses given by dashes.

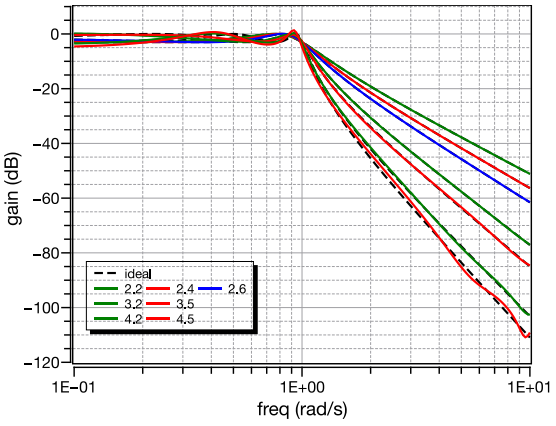

FIGURE 2. Frequency responses of the approximated Chebyshev low-pass filters with the ideal responses given by dashes.

2) HIGH-PASS FILTER FUNCTIONS

The magnitude response of high-pass fractional filters with Butterworth characteristics is given in (4)

$$\left|H_{HP,n+\alpha}(\omega)\right| = \frac{1}{\sqrt{1 + \left(\frac{\omega_0}{\omega}\right)^{2(n+\alpha)}}}, \quad (4)$$

TABLE 1. Coefficients values of (3) for approximating Butterworth low-pass filters of orders {2.2, 2.4, 2.6}, {3.2, 3.5}, and {4.2, 4.5}.

Coefficient	Order						
	2.2	2.4	2.6	3.2	3.5	4.2	4.5
B_4	0.001814	0.002064	0.001779	0.0002597	0.0000312	0.000114	0.0001172
B_3	0.04282	0.03649	0.02766	0.007002	0.00284	0.001621	0.001168
B_2	0.8219	0.5933	0.4192	0.1082	0.04011	0.0261	0.02113
B_1	2.678	2.13	1.726	0.9779	0.5232	0.1732	0.1077
B_0	0.9283	0.8394	0.8468	2.338	1.561	0.8481	0.6357
A_3	4.179	3.685	3.328	4.249	3.425	2.351	1.904
A_2	5.662	4.815	4.316	6.541	4.788	3.025	2.503
A_1	4.032	3.426	3.108	5.591	3.896	2.252	1.717
A_0	0.9275	0.8378	0.8451	2.335	1.56	0.846	0.6439

TABLE 2. Coefficients values of (3) for approximating Chebyshev low-pass filters of orders {2.2, 2.4, 2.6}, {3.2, 3.5}, and {4.2, 4.5}.

Coefficient	Order						
	2.2	2.4	2.6	3.2	3.5	4.2	4.5
B_4	0.001221	0.0009494	0.0006014	0.0000436	0.0000088	0.0000356	0.0000325
B_3	0.02356	0.01521	0.009347	0.001662	0.0009599	0.0002777	0.0001289
B_2	0.3763	0.2336	0.1398	0.02029	0.008234	0.00511	0.004082
B_1	1.057	0.7784	0.5737	0.1937	0.106	0.02182	0.009537
B_0	0.4116	0.3493	0.3115	0.2153	0.1621	0.1129	0.09124
A_3	2.979	2.565	2.222	1.279	0.8642	0.5143	0.4011
A_2	2.834	2.336	1.988	1.377	1.233	1.143	1.087
A_1	2.219	1.889	1.636	0.9373	0.6174	0.3537	0.2704
A_0	0.582	0.4732	0.3884	0.2046	0.1702	0.1762	0.1628

and the corresponding expression of the Chebyshev high-pass filters is

$$\left|H_{HP,n+\alpha}(\omega)\right| = \frac{1}{\sqrt{1+\varepsilon^2 C^2_{n+\alpha}(\omega)}}, \tag{5}$$

with $C_{n+\alpha}(\omega) = cos\left[(n+\alpha)\cdot cos^{-1}\left(\frac{\omega_0}{\omega}\right)\right]$.

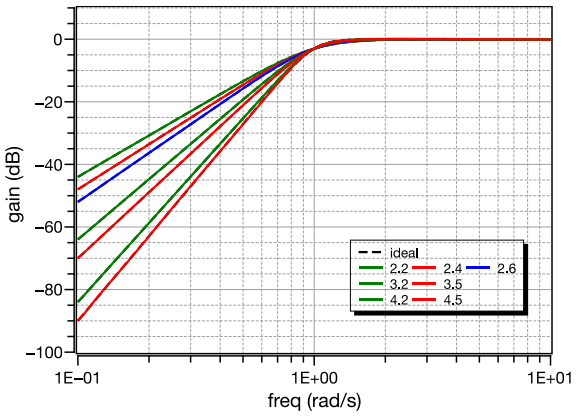

FIGURE 3. Frequency responses of the approximated Butterworth high-pass filters with the ideal responses given by dashes.

Following the same procedure in the case of high-pass filters described by (4)–(5), the resulting values of coefficients are given in Tables 3–4. The associated frequency responses are demonstrated in Figs. 3 and 4, respectively.

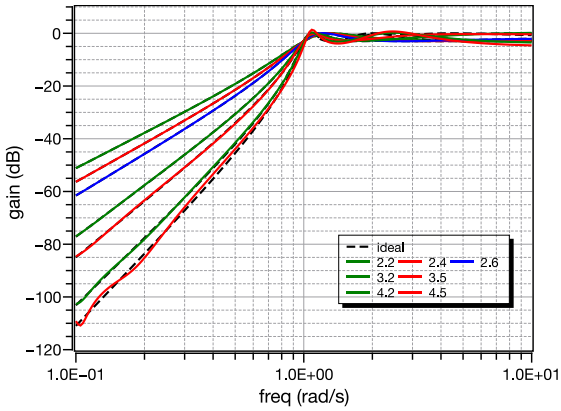

FIGURE 4. Frequency responses of the approximated Chebyshev high-pass filters of orders {2.2, 2.,4, 2.6} with the ideal responses given by dashes.

3) BAND-PASS FILTER FUNCTIONS

The expression of the magnitude of a Butterworth band-pass filter of order $(n+\alpha)$ is given by (6)

$$\left|H_{BP,n+\alpha}(\omega)\right| = \frac{1}{\sqrt{1+\left(\frac{|\omega_0^2-\omega^2|}{\omega\cdot BW}\right)^{2(n+\alpha)}}}, \tag{6}$$

with ω_0 being the center frequency and BW is the bandwidth of the filter ($BW = \omega_{high} - \omega_{low}$). Considering a band-pass frequency response with $\omega_0 = 1$ rad/s, $\omega_{low} = \omega_o/2$ and $\omega_{high} = 2\omega_0$, the values of coefficients which are associated with filters of orders {2.2, 2.4, 2.6} are given in Table 5.

TABLE 3. Coefficients values of (3) for approximating Butterworth high-pass filters of orders {2.2, 2.4, 2.6}, {3.2, 3.5}, and {4.2, 4.5}.

Coefficient	Order						
	2.2	2.4	2.6	3.2	3.5	4.2	4.5
B_4	1.001	1.002	1.002	1	1.001	0.9959	0.991
B_3	2.888	2.542	2.042	0.5141	0.3349	0.1998	0.169
B_2	0.8861	0.7082	0.4961	0.04617	0.02872	0.02851	0.03409
B_1	0.04617	0.04355	0.03273	0.002982	0.001994	0.001755	0.001889
B_0	0.001955	0.002464	0.002105	0.0000619	0.0000406	0.0001139	0.0001969
A_3	4.347	4.089	3.678	2.504	2.491	2.644	2.683
A_2	6.105	5.748	5.106	3.054	3.043	3.589	3.86
A_1	4.505	4.399	3.937	2.1	2.176	2.764	2.972
A_0	1.078	1.194	1.183	0.576	0.6218	1.198	1.529

TABLE 4. Coefficients values of (3) for approximating Chebyshev high-pass filters of orders {2.2, 2.4, 2.6}, {3.2, 3.5}, and {4.2, 4.5}.

Coefficient	Order						
	2.2	2.4	2.6	3.2	3.5	4.2	4.5
B_4	0.7072	0.7383	0.802	1.053	0.9522	0.6408	0.56
B_3	1.817	1.645	1.477	0.9475	0.6228	0.1242	0.05835
B_2	0.6466	0.4936	0.3599	0.09918	0.04834	0.02898	0.0251
B_1	0.04049	0.03215	0.02407	0.008124	0.005637	0.00158	0.0007885
B_0	0.002098	0.00201	0.001548	0.0002132	0.0000515	0.0002017	0.0002
A_3	3.813	3.992	4.212	4.582	3.627	2.002	1.665
A_2	4.87	4.937	5.118	6.735	7.244	6.499	6.667
A_1	5.118	5.42	5.723	6.252	5.076	2.912	2.468
A_0	1.718	2.113	2.575	4.891	5.874	5.69	6.128

TABLE 5. Coefficients values of (3) for approximating Butterworth band-pass filters of orders {2.2, 2.4, 2.6}.

Coefficient	Order		
	2.2	2.4	2.6
B_4	0.01429	0.01631	0.01603
B_3	0.1472	0.11	0.07758
B_2	1.994	1.739	1.506
B_1	0.1472	0.11	0.07758
B_0	0.01429	0.01631	0.01603
A_3	1.83	1.561	1.312
A_2	3.996	3.774	3.586
A_1	1.83	1.561	1.312
A_0	1	1	1

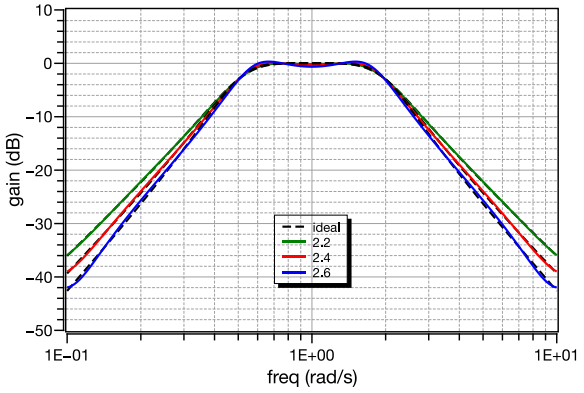

FIGURE 5. Frequency response of the approximated Butterworth band-pass filters with the ideal responses given by dashes.

The corresponding plots of the frequency responses plots are demonstrated in Fig. 5.

From the above, it is obvious that the proposed method offers the following advantages:

- It is versatile, in the sense that it is applicable in various types of filters functions (i.e., low-pass, high-pass, band-pass) and is independent of the type of the polynomial that is used for the prototype filter (e.g. Butterworth and Chebyshev).
- It is very simple because, having available the frequency response of the filter, one step is required to obtain the rational integer-order transfer function which approximates the fractional-order filter function.
- It offers design flexibility and programmability since the transfer function in (3) is used for implementing the derived transfer functions of all types, i.e. the same core can be used for implementing different filters.

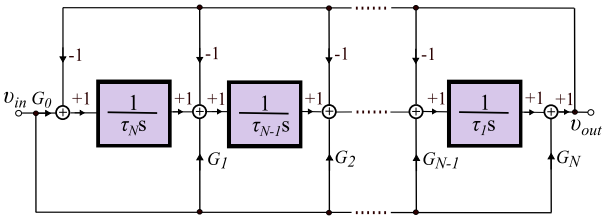

FIGURE 6. Functional block diagram of an n^{th}–order Inverse Follow the Leader Feedback structure.

III. IMPLEMENTATIONS

A. ELECTRONICALLY CONTROLLED IMPLEMENTATION

The transfer function in (3) can be realized using an Inverse Follow the Leader Feedback (IFLF) topology, described by

the functional block diagram in Fig. 6 [30]. The realized transfer function in this case is (7)

$$H(s) = \frac{G_n s^N + \frac{G_{N-1}}{\tau_1} s^{N-1} + \cdots + \frac{G_0}{\tau_1 \tau_2 \cdots \tau_{N-1} \tau_N}}{s^N + \frac{1}{\tau_1} s^{N-1} + \cdots + \frac{1}{\tau_1 \tau_2 \cdots \tau_{N-1} \tau_N}}, \quad (7)$$

and the values of time-constants as well of scaling factors are calculated by equalizing the coefficients of (3) and (7). The resulting design equations are thus (8)–(9)

$$\tau_{i+1} = \frac{A_{N-i}}{A_{N-1-i}} (i = 0 \ldots N-1), \quad (8)$$

$$G_j = \frac{B_j}{A_j} (j = 0 \ldots N). \quad (9)$$

The corresponding OTA-C structure, which implements the block diagram in Fig. 6, in the case of a 4$^{\text{th}}$–order approximation, is depicted in Fig. 7(a). The circuitry shown in Fig. 7(b) could be utilized for realizing the required OTAs, due to the offered improved linearity compared to that offered by conventional implementations [31]. Its small-signal transconductance parameter is given by $g_m = \frac{5I_B}{9nV_T}$ with n being the slope factor of a MOS transistor in sub-threshold region ($1 < n < 2$), V_T being the thermal voltage (26 mV at 27° C), and I_B being the dc bias current. Consequently, the time-constant of each integration stage $\tau_i = C_i/g_{mi}$ ($i = 1,2 \ldots 4$) is controlled by the dc bias current of the associated OTAs; in addition, the scaling factors G_j ($j = 0,1 \ldots 4$) are implemented by scaling the dc bias currents of the OTAs employed for performing this operation.

Using the values of Tables 1–4, the design equations in (8)–(9) and denormalizing frequency to $\omega_0 = 1$ krad/s, the derived values of the bias currents of the integration sections are given in Table 6 in the case of Butterworth filters, and in Table 7 in the case of Chebyshev filters. In both cases the main bias current of the summation stages is equal to 98.3 nA.

TABLE 6. Values of dc bias currents for approximating Butterworth low-pass, high-pass, and band-pass filters of orders {2.2, 2.4, 2.6}, using the structure in Fig. 7.

Filter	Order	I_{B1}	I_{B2}	I_{B3}	I_{B4}
LP	**2.2**	20 nA	914 pA	17.7 nA	680 nA
	2.4	18.4 nA	860 pA	17.9 nA	735 nA
	2.6	15 nA	910 pA	17.3 nA	986 nA
HP	**2.2**	24.5 nA	980 pA	18.4 nA	827 nA
	2.4	20.7 nA	950 pA	20 nA	745 nA
	2.6	20.1 nA	916 pA	22 nA	843.8 nA
BP	**2.2**	10.02 nA	2.146 nA	14.146 nA	1.53 µA
	2.4	8.549 nA	2.375 nA	12.778 nA	1.799 µA
	2.6	7.182 nA	2.687 nA	11.299 nA	2.141 µA

B. DIGITALLY CONTROLLED IMPLEMENTATION

Another possible implementation of the transfer function in (3) is that based on the functional block diagram in Fig. 8, which represents a Follow the Leader Feedback (FLF) structure [32]. The realized transfer function is the same as that in (7) and, therefore, the design equations (8)–(9) are still valid. Its implementation can be performed using the FPAA AN231E04 device provided by Anadigm [33]. The internal intermediate blocks are interconnected through programmable buses and this offers attractive design flexibility and versatility [34], [35].

TABLE 7. Values of dc bias currents for approximating Chebyshev low-pass and high-pass filters of orders {2.2, 2.4, 2.6}, using the structure in Fig. 7.

Filter	Order	I_{B1}	I_{B2}	I_{B3}	I_{B4}
LP	**2.2**	14.6 nA	620 pA	20.5 nA	735 nA
	2.4	12 nA	595 pA	21.1 nA	702 nA
	2.6	10 nA	600 pA	21.1 nA	666 nA
HP	**2.2**	20.9 nA	807 pA	29.6 nA	942.7 nA
	2.4	21.9 nA	748 pA	32.5 nA	1.1 µA
	2.6	23.5 nA	710 pA	36 nA	1.3 µA

The integration constants (M_i) are formed as $M_i = 10^{-6}/\tau_i$ ($i = 1 \ldots 4$), having units of μs^{-1}. Choosing the FPAA clock frequency as $f_{clk} = 2$ MHz, then the realizable weight factor values of summation stages which implement the scaling factors G_j ($j = 0,1 \ldots 4$) are in the range [0.01, 8.83]. This is due to the switched-capacitor nature of operation of the FPAA and some values of these G_j factors are not in the realizable range. However, this problem can be overcome by adding one extra gain stage at the input of the summation stages with a value given by the formula: $G = \sqrt{G_j}$, ($j = 0 \ldots 4$). Moreover, the values of the inherit gain of the inputs of the summation stages will become equal to that of the associated extra gain stage (i.e.,$\sqrt{G_j}$), for ensuring that the total gain across the path is equal to that of the associated scaling factor. Following this, the resulting design obtained using the *Anadigm Designer®2* EDA software is demonstrated in Fig. 15, where the corresponding experiment implementation is also provided. The interface is used for performing the single-to-differential conversion of the input signal, as well as, the differential-to-single-ended conversion of the output signal. The parameters of *"GainHold" (gain stage) and "Integrator"* Configurable Analogue Modules (CAMs) for implementing low and high-pass filters with cutoff frequency equal to 100 krad/s, as well as band-pass filter with the same center frequency employing a 4$^{\text{th}}$–order approximation, are provided in Tables 8–9, respectively.

IV. SIMULATIONS AND EXPERIMENTAL RESULTS

A. SIMULATION RESULTS

The performance of the topology in Fig. 7(a) will be evaluated using the Cadence IC design suite and the Austria Mikro Systeme (AMS) CMOS 0.35 µm design kit. Considering a dc bias voltages scheme $V_{DD} = -V_{SS} = 0.75$ V and that the MOS transistors are biased at the sub-threshold region, their chosen aspect ratios are provided in Table 10. The layout design of the OTA is demonstrated in Fig. 9. The post-layout frequency responses of Butterworth and Chebyshev filters of orders {2.2. 2.4, 2.6} are depicted in Figs. 10 and 11, respectively. The frequency responses of the band-pass filters are provided

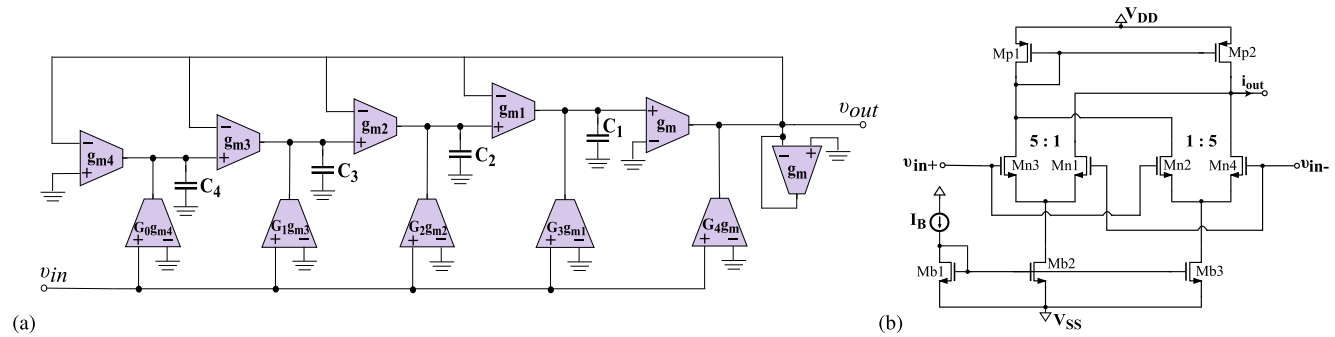

FIGURE 7. (a) OTA-C implementation of the functional block diagram in Fig. 6, in the case of 4th–order approximation and (b) OTA internal structure.

TABLE 8. Values of integration constants (μs^{-1}) and gain factors for implementing Butterworth band-pass filters of orders {2. 2, 2.4, 2.6}.

Stage	Order		
	2.2	2.4	2.6
M_1, M_2, M_3, M_4	0.183, 0.218, 0.0458, 0.0546	0.156, 0.242, 0.0414, 0.0640	0.131, 0.273, 0.0366, 0.0762
$\sqrt{G_0}$,$\sqrt{G_1}$,$\sqrt{G_2}$,$\sqrt{G_3}$, $\sqrt{G_4}$	0.12, 0.284, 0.706, 0.284, 0.12	0.128, 0.265, 0.679, 0.265, 0.128	0.127, 0.243, 0.648, 0.243, 0.127

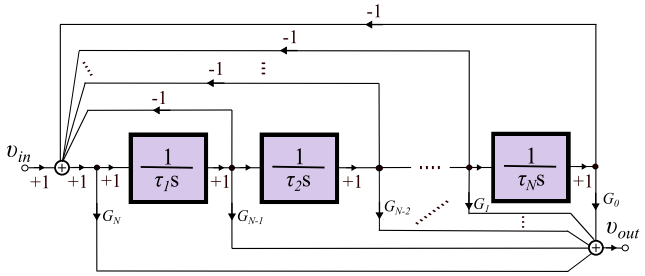

FIGURE 8. Functional block diagram of an *n*th–order Follow the Leader Feedback structure.

TABLE 9. Values of integration constants (μs^{-1}) and gain factors for implementing Butterworth low-pass and high-pass filters of orders {4.2, 4.5}.

Stage	Low-pass		High-pass	
	4.2	4.5	4.2	4.5
M_1	0.231	0.193	0.266	0.268
M_2	0.129	0.129	0.134	0.144
M_3	0.0737	0.0695	0.0776	0.0769
M_4	0.0378	0.0369	0.0427	0.0516
$\sqrt{G_0}$	1	1	0.0104	0.0110
$\sqrt{G_1}$	0.2766	0.2496	0.0260	0.0249
$\sqrt{G_2}$	0.090	0.0930	0.0920	0.0935
$\sqrt{G_3}$	0.0256	0.0248	0.2768	0.2499
$\sqrt{G_4}$	0.011	0.0110	1	1

in Fig. 12, while their important frequency characteristics are summarized in Table 11.

TABLE 10. Aspect ratios of the MOS transistors in Fig. 7(b).

Transistors	Aspect-ratio
M_{b1}-M_{b3}	4.4 μm/5 μm
M_{p1}-M_{p2}	0.5 μm/1.5 μm
M_{n1}-M_{n2}	1.1 μm/1.5 μm
M_{n3}-M_{n4}	5.5 μm/1.5 μm

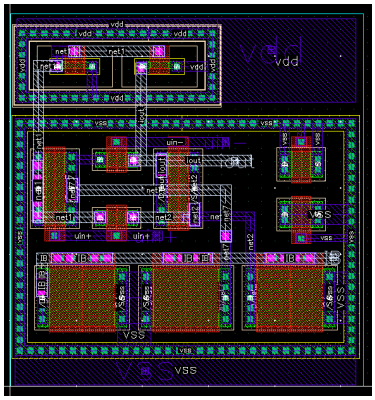

FIGURE 9. Layout design of the OTA structure in Fig.7(b).

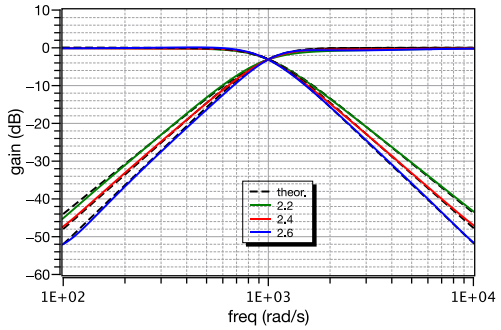

FIGURE 10. Post-layout frequency responses of the designed low-pass and high-pass Butterworth filters of orders {2.2, 2.4, 2.6}.

TABLE 11. Frequency characteristics of the designed Butterworth band-pass filters, obtained through simulations.

Parameter	Theory	Fractional-order $n + \alpha$		
		2.2	2.4	2.6
ω_{low}(krad/s)	0.5	0.498	0.499	0.502
ω_{high}(krad/s)	2	2	2	1.992
Bandwidth (krad/s)	1.5	1.502	1.501	1.490
ω_0(krad/s)	1	0.998	0.999	1

The time-domain behavior of the filters has been evaluated for the case of a Butterworth low-pass filter of order equal to 2.4. For this purpose, a (50 mV, 1 krad/s) sinusoidal stimulus is applied to the filter and the obtained waveforms are

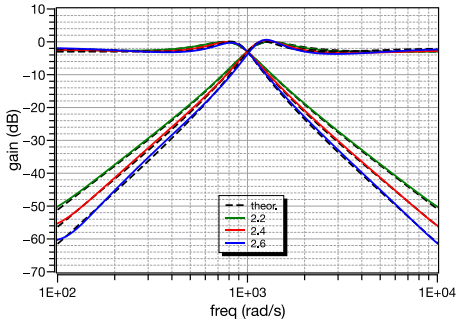

FIGURE 11. Post-layout frequency responses of the designed low-pass and high-pass Chebyshev filters of orders {2.2, 2.4, 2.6}.

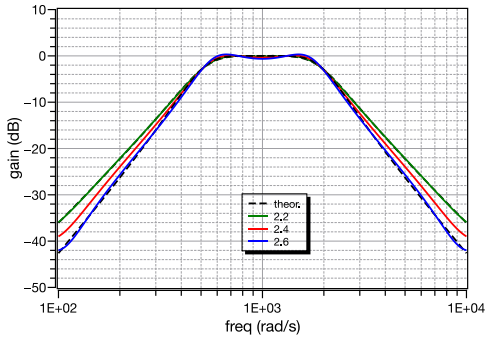

FIGURE 12. Post-layout frequency responses of the designed band-pass Butterworth filters of orders {2.2, 2.4, 2.6}.

demonstrated in Fig. 13(a), where the measured value of the gain is −3.01 dB, close to the theoretically predicted value of −3 dB.

The linearity of the filter has been evaluated through a 62.8 rad/s stimulus of variable amplitude, and the Total Harmonic Distortion (THD) versus amplitude plot are depicted in Fig. 13(b). THD levels of 1% and 2% are observed at 52 mV and 73.5 mV amplitudes, respectively. Integrating the noise over the pass-band of the filter, the *rms* value of the input referred noise was 42.6 μV. Consequently, the predicted value of the Dynamic Range (DR) of the filter (at 1% THD level) is equal to 58.72 dB.

The sensitivity of the filters has been evaluated through the utilization of Monte-Carlo analysis for $N = 500$ runs. The obtained statistical distribution of the cutoff frequency and bandwidth of the Butterworth low-pass and band-pass filters of order 2.4 are demonstrated in Figs. 14(a, b). The corresponding values of the standard deviation are 104.32 rad/s and 24.1 rad/s, respectively, and taking into account that the associated mean values are 1.02 krad/s and 1.496 krad/s, it is concluded that the introduced topology offers reasonable sensitivity characteristics.

B. EXPERIMENTAL RESULTS

The frequency responses of the Butterworth band-pass filters of orders {2.2, 2.4, 2.6}, and of low/high-pass filters of orders {4.2, 4.5} obtained using the HP4395A Network/Impedance analyzer are given in Figs. 16(a, b). The

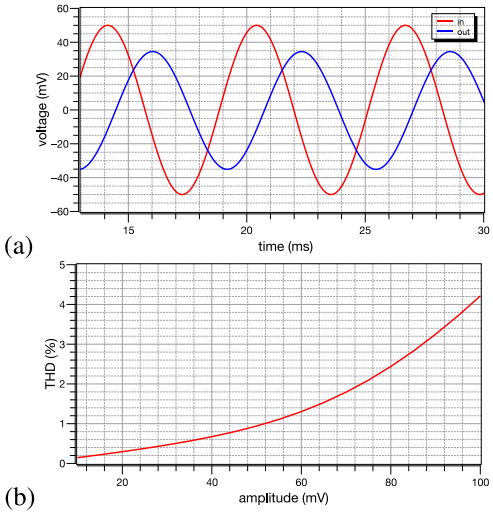

FIGURE 13. (a) Time-domain post-layout frequency responses of the designed Butterworth low-pass filter (order 2.4) for a (50 mV, 1 krad/s) stimulus and (b) its linearity performance using a 62.8 rad/s stimulus of variable amplitude.

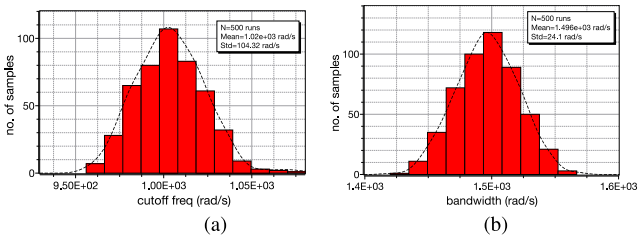

FIGURE 14. Statistical plots of the Butterworth low-pass filter of order 2.4 (a) cutoff frequency and (b) bandwidth.

TABLE 12. Frequency characteristics of the implemented Butterworth band-pass filters, obtained through measurements.

Parameter	Theory	Fractional-order $n + \alpha$		
		2.2	2.4	2.6
ω_{low}(krad/s)	50	49.9	49.7	49.8
ω_{high}(krad/s)	200	197.33	197.64	197.55
Bandwidth (krad/s)	150	147.43	147.94	147.75
ω_0(krad/s)	100	99.2	99.11	99.19

values of the cutoff frequency of the low-pass filters of order 4.2 and 4.5 were measured as 99.1 krad/s and 98.2 krad/s, respectively. In the case of the high-pass filters, the derived values were 101.1 krad/s and 101.8 krad/s which are all close to the theoretical value of 100 krad/s. The measured values of the frequency characteristics of the band-pass filters are summarized in Table 12.

The time-domain behavior of the filters has been evaluated as follows: the band-pass filter of order 2.6 is stimulated by a 1Vp-p sinusoidal signal with frequency equal to the upper cutoff frequency (i.e., 197.55 krad/s), while the low-pass filter was stimulated by a 1 Vp-p sinusoidal signal with frequency corresponding to the cutoff frequency of the filters (i.e. 98.2 krad/s). Using a DSO6034A oscilloscope, the resulting screenshots are demonstrated in Figs. 17(a, b).

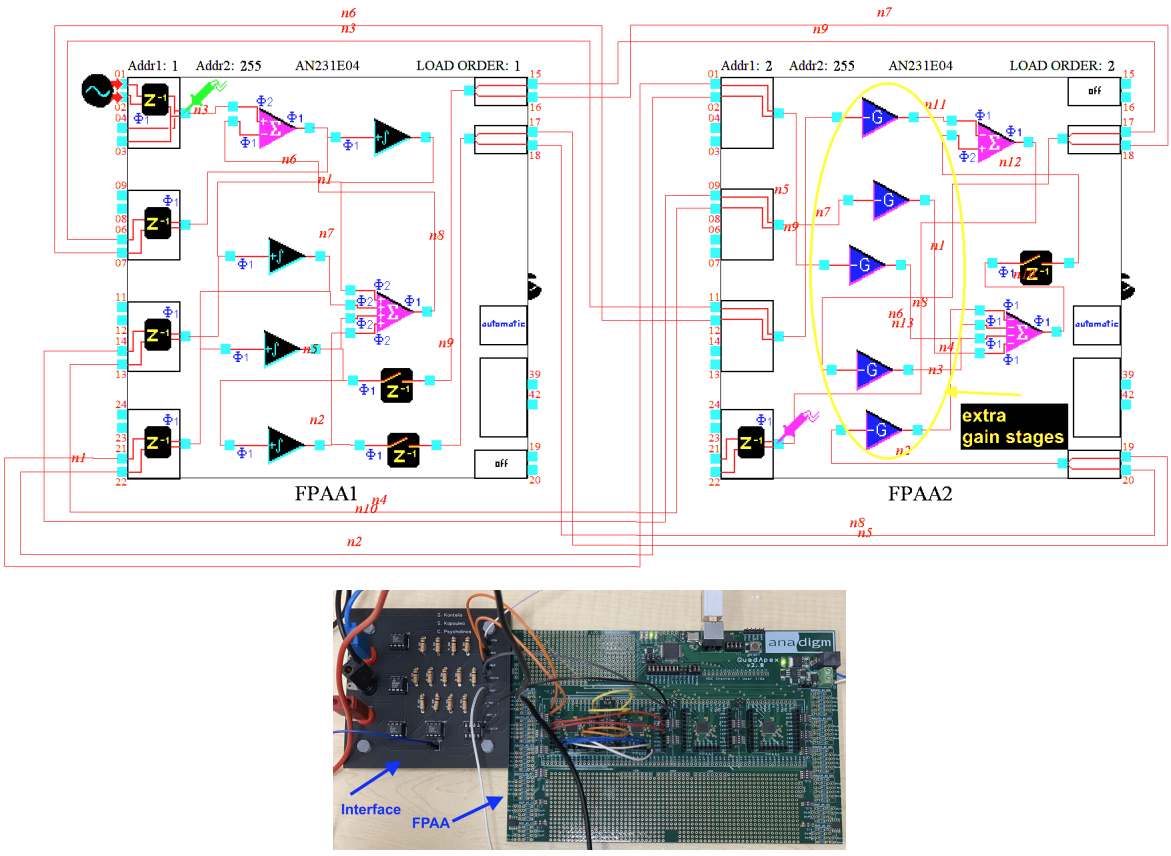

FIGURE 15. FPAA configuration for realizing fractional-order filters (4th–order approximation) and its corresponding implementation.

The values of the measured gains were −2.8dB and −2.85dB, close to the theoretical −3dB value.

Finally, the linear performance of the implemented filters was evaluated in the case of a low-pass filer of order 4.5, stimulated by a 6.28 krad/s signal with the amplitude set to the maximum allowable by the FPAA (i.e., 3 Vp-p). The second harmonic was found at 77.65 dB below the fundamental.

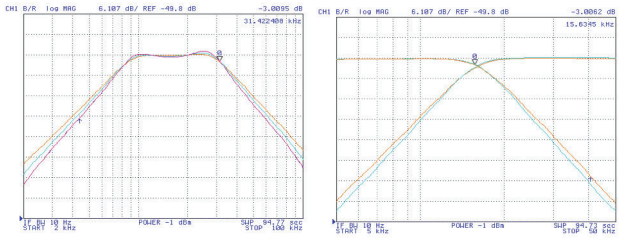

(a) (b)

FIGURE 16. Experimental frequency responses of the Butterworth (a) band-pass filters of orders {2.2, 2.4, 2.6} and (b) low-pass/high-pass filters of orders {4.2, 4.5} realized using the FPAA configuration in Fig. 15.

With regards to the presented implementations which both offer adjustability of the derived frequency characteristics of the realized filter functions, the OTA-C structure offers the following benefits: a) capability of monolithic implementation on silicon, and b) greater maximum frequency of operation than that offered by the FPAA

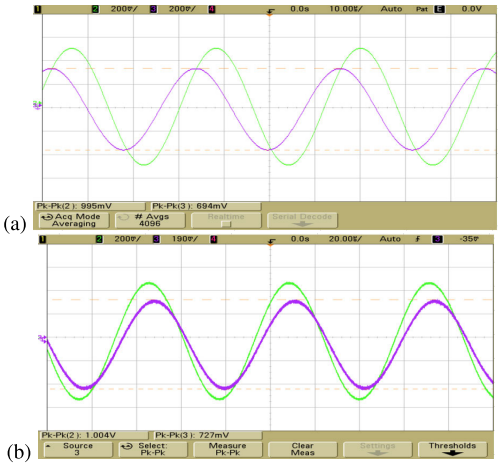

(a) (b)

FIGURE 17. Experimental input and output waveforms of a (a) band-pass filter of order 2.6, stimulated by a (1Vp-p, 197.55krad/s) sinusoidal signal and (b) low-pass filter of order 4.5 stimulated by a (1Vp-p, 98.2krad/s).

implementation. This is due to the absence of a compensation network in the internal structure of the OTA, by contrast to the FPAA device where internally compensated op-amps are used as active elements.

Another imposed restriction on the maximum frequency of operation of the FPAA structure is due to the fact that the switched-capacitor technique is used for implementing the signal processing. The maximum allowed clock frequency in the presented design was 2 MHz, restricting the maximum

frequency of (accurate) operation to the order of few kHz. On the other hand, the employment of the small-signal transconductance parameter (g_m) of OTAs for realizing the required time-constants and scaling factors imposes restriction on the maximum amplitude of the signal that can be handled by the system with a low level of distortion. This is obvious from the provided results, where THD levels of 1% and 2% are observed at 52 mV and 73.5 mV, respectively. The FPAA implementation does not suffer from this obstacle, because of the employment of op-amps. This is evident from the provided results where, for a 1.5 V amplitude, the second harmonic was found to be 77.65 dB below the fundamental tone.

With regards to the dc power dissipation, considering a band-pass filter of order equal to 2.4, the corresponding values are 3.88 μW for the OTA-C realization and 430 mW for the FPAA implementation. The increased power dissipation of the FPAA structure is the price paid for its better linear performance, compared to that offered by the OTA-C filter.

V. CONCLUSION

A systematic way for deriving rational integer-order transfer functions which approximate the behavior of fractional filters of order greater than two was presented in this paper. This is actually a two-step procedure based on the fitting of the magnitude response of the desired fractional-order filter function. In this work, the chosen order of approximation was equal to four in order to achieve an accurate level of approximation. The procedure is versatile in the sense that it is independent from the order as well as from the type of filter. For demonstration purposes, Butterworth and Chebyshev filter responses have been implemented in this work, but the procedure is also applicable to other types such as inverse Chebyshev, Bessel or Elliptic filters. It is noticeable that this procedure preserves the cutoff frequency of the approximated filters unlike the methods of [5] and [9] and without using any complex algorithms as in [7], [22], [25], [26], and [27]. We have provided robust implementations to validate the designed higher-order filters on the integrated circuit level (using CMOS OTAs) and experimentally using a switched-C based FPAA platform.

ACKNOWLEDGMENT

The publication of the article in OA mode was financially supported by HEAL-Link.

REFERENCES

[1] C. I. Muresan, I. R. Birs, E. H. Dulf, D. Copot, and L. Miclea, "A review of recent advances in fractional-order sensing and filtering techniques," *Sensors*, vol. 21, no. 17, p. 5920, Sep. 2021.

[2] N. Mijat, D. Jurisic, and G. S. Moschytz, "Analog modeling of fractional-order elements: A classical circuit theory approach," *IEEE Access*, vol. 9, pp. 110309–110331, 2021.

[3] G. Tsirimokou, "A systematic procedure for deriving RC networks of fractional-order elements emulators using MATLAB," *AEU-Int. J. Electron. Commun.*, vol. 78, pp. 7–14, Aug. 2017.

[4] G. Tsirimokou, C. Psychalinos, and A. S. Elwakil, "Fractional-order electronically controlled generalized filters," *Int. J. Circuit Theory Appl.*, vol. 45, no. 5, pp. 595–612, May 2017.

[5] T. J. B. Freeborn, B. Maundy, and A. S. Elwakil, "Field programmable analogue array implementation of fractional step filters," *IET Circuits Devices Syst.*, vol. 4, no. 6, pp. 514–524, Nov. 2010.

[6] B. Maundy, A. S. Elwakil, and T. J. Freeborn, "On the practical realization of higher-order filters with fractional stepping," *Signal Process.*, vol. 91, no. 3, pp. 484–491, 2011.

[7] T. Freeborn, B. Maundy, and A. S. Elwakil, "Approximated fractional order Chebyshev lowpass filters," *Math. Problems Eng.*, vol. 2015, pp. 1–7, Mar. 2015.

[8] T. J. Freeborn, A. S. Elwakil, and B. Maundy, "Approximated fractional-order inverse Chebyshev lowpass filters," *Circuits, Syst., Signal Process.*, vol. 35, no. 6, pp. 1973–1982, Jun. 2016.

[9] T. J. Freeborn, "Comparison of (1+ α) fractional-order transfer functions to approximate lowpass Butterworth magnitude responses," *Circuits, Syst., Signal Process.*, vol. 35, no. 6, pp. 1983–2002, 2016.

[10] S. Mahata, S. K. Saha, R. Kar, and D. Mandal, "Optimal design of fractional order low pass Butterworth filter with accurate magnitude response," *Digit. Signal Process.*, vol. 72, pp. 96–114, Jan. 2018.

[11] D. Kubanek, T. J. Freeborn, J. Koton, and J. Dvorak, "Validation of fractional-order lowpass elliptic responses of (1+ α)-order analog filters," *Appl. Sci.*, vol. 8, no. 12, p. 2603, 2018.

[12] D. Kubanek and T. Freeborn, "(1+α) fractional-order transfer functions to approximate low-pass magnitude responses with arbitrary quality factor," *AEU-Int. J. Electron. Commun.*, vol. 83, pp. 570–578, Jan. 2018.

[13] L. Langhammer, R. Sotner, J. Dvorak, and T. Dostal, "Fully-differential multifunctional electronically configurable fractional-order filter with electronically adjustable parameters," *Elektronika Elektrotechnika*, vol. 24, no. 5, pp. 42–45, Oct. 2018.

[14] D. Kubanek, T. Freeborn, and J. Koton, "Fractional-order band-pass filter design using fractional-characteristic specimen functions," *Microelectron. J.*, vol. 86, pp. 77–86, Apr. 2019.

[15] A. M. Abdelaty, A. Soltan, W. A. Ahmed, and A. G. Radwan, "Fractional order Chebyshev-like low-pass filters based on integer order poles," *Microelectron. J.*, vol. 90, pp. 72–81, Aug. 2019.

[16] S. Mahata, R. Kar, and D. Mandal, "Optimal fractional-order highpass Butterworth magnitude characteristics realization using current-mode filter," *AEU-Int. J. Electron. Commun.*, vol. 102, pp. 78–89, Apr. 2019.

[17] S. Mahata, S. Saha, R. Kar, and D. Mandal, "Optimal integer-order rational approximation of α and $\alpha + \beta$ fractional-order generalised analogue filters," *IET Signal Process.*, vol. 13, no. 5, pp. 516–527, Jul. 2019.

[18] S. Mahata, S. Banerjee, R. Kar, and D. Mandal, "Revisiting the use of squared magnitude function for the optimal approximation of (1+ α)-order Butterworth filter," *AEU-Int. J. Electron. Commun.*, vol. 110, Oct. 2019, Art. no. 152826.

[19] A. Soni and M. Gupta, "Analysis and design of optimized fractional order low-pass Bessel filter," *J. Circuits, Syst. Comput.*, vol. 30, no. 2, Feb. 2021, Art. no. 2150035.

[20] S. Shrivastava, D. K. Upadhyay, and O. P. Goswami, "Optimal design of fractional-order low-pass filter using L2-method," in *Proc. Int. Conf. Commun., Control Inf. Sci. (ICCISc)*, vol. 1, Jun. 2021, pp. 1–5.

[21] L. Langhammer, R. Sotner, J. Dvorak, J. Jerabek, and D. Andriukaitis, "Reconnection–less reconfigurable fractional–order current–mode integrator design with simple control," *IEEE Access*, vol. 9, pp. 136395–136405, 2021.

[22] S. Mahata, N. Herencsar, D. Kubanek, and I. C. Goknar, "Optimized fractional-order Butterworth filter design in complex F-plane," *Fractional Calculus Appl. Anal.*, vol. 25, no. 5, pp. 1801–1817, Oct. 2022.

[23] S. Mahata, R. Kar, and D. Mandal, "Optimal design of fractional-order Butterworth filter with improved accuracy and stability margin," in *Fractional-Order Modeling of Dynamic Systems with Applications in Optimization, Signal Processing, and Control*. Amsterdam, The Netherlands: Elsevier, 2022, pp. 293–321.

[24] A. Soni and M. Gupta, "Designing of fractional order Bessel filter using optimization techniques," *Int. J. Electron. Lett.*, vol. 10, no. 1, pp. 71–86, Jan. 2022.

[25] O. Sladok, J. Koton, D. Kubanek, J. Dvorak, and C. Psychalinos, "Pseudo-differential (2+α)-order Butterworth frequency filter," *IEEE Access*, vol. 9, pp. 92178–92188, 2021.

[26] D. Kubanek, J. Koton, J. Jerabek, and D. Andriukaitis, "(n+α)-order low-pass and high-pass filter transfer functions for non-cascade implementations approximating Butterworth response," *Fractional Calculus Appl. Anal.*, vol. 24, no. 3, pp. 689–714, Jun. 2021.

[27] X. He and Z. Hu, "Optimization design of fractional-order Chebyshev lowpass filters based on genetic algorithm," *Int. J. Circuit Theory Appl.*, vol. 50, no. 5, pp. 1420–1441, May 2022.
[28] J. Valsa and J. Vlach, "RC models of a constant phase element," *Int. J. Circuit Theory Appl.*, vol. 41, no. 1, pp. 59–67, 2013.
[29] R. Daryani, B. Aggarwal, and M. Gupta, "Design of fractional-order Chebyshev low-pass filter for optimized magnitude response using meta-heuristic evolutionary algorithms," *Circuits, Syst., Signal Process.*, vol. 42, pp. 1–31, Nov. 2022.
[30] G. Tsirimokou, C. Psychalinos, A. S. Elwakil, and K. N. Salama, "Electronically tunable fully integrated fractional-order resonator," *IEEE Trans. Circuits Syst. II, Exp. Briefs*, vol. 65, no. 2, pp. 166–170, Feb. 2018.
[31] P. Corbishley and E. Rodriguez-Villegas, "A nanopower bandpass filter for detection of an acoustic signal in a wearable breathing detector," *IEEE Trans. Biomed. Circuits Syst.*, vol. 1, no. 3, pp. 163–171, Sep. 2007.
[32] G. Tsirimokou, C. Psychalinos, and A. Elwakil, *Design of CMOS Analog Integrated Fractional-Order Circuits: Applications in Medicine and Biology*. Cham, Switzerland: Springer, 2017.
[33] Anadigm. *AN231E04 dpASP: The AN231E04 dpASP Dynamically Reconfigurable Analog Signal Processor*. Accessed: May 3, 2023. [Online]. Available: https://www.anadigm.com/an231e04.asp
[34] C. Muñiz-Montero, L. V. García-Jiménez, L. A. Sánchez-Gaspariano, C. Sánchez-López, V. R. González-Díaz, and E. Tlelo-Cuautle, "New alternatives for analog implementation of fractional-order integrators, differentiators and PID controllers based on integer-order integrators," *Nonlinear Dyn.*, vol. 90, no. 1, pp. 241–256, 2017.
[35] E. Tlelo-Cuautle, A. D. Pano-Azucena, O. Guillén-Fernández, and A. Silva-Juárez, *Analog/Digital Implementation of Fractional Order Chaotic Circuits and Applications*. Cham, Switzerland: Springer, 2020.

JULIA NAKO (Graduate Student Member, IEEE) received the B.Sc. and M.Sc. degrees from the University of Patras, Greece, in 2021 and 2023, respectively, where she is currently pursuing the Ph.D. degree in electronics-circuits and systems with the Physics Department. She is a member of the Analog VLSI Design Team, Electronics Laboratory, working under the supervision of Prof. Costas Psychalinos. Her research interests include the design of analog integrated circuits and systems for signal processing, including non-integer order circuits, control systems, and biomedical circuits.

COSTAS PSYCHALINOS (Senior Member, IEEE) received the B.Sc. and Ph.D. degrees in physics and electronics from the University of Patras, Greece, in 1986 and 1991, respectively. From 1993 to 1995, he was a Postdoctoral Researcher with the VLSI Design Laboratory, University of Patras. From 1996 to 2000, he was an Adjunct Lecturer with the Department of Computer Engineering and Informatics, University of Patras. From 2000 to 2004, he was an Assistant Professor with the Electronics Laboratory, Department of Physics, Aristotle University of Thessaloniki, Greece. Since 2004, he has been a Faculty Member with the Electronics Laboratory, Department of Physics, University of Patras, where he is currently a Full Professor. His research interests include the development of CMOS analog integrated circuits, including fractional-order circuits and systems, continuous and discrete-time analog filters, amplifiers, and low-voltage/low-power building blocks for analog signal processing. He is a member of the Nonlinear Circuits and Systems Technical Committee of the IEEE CAS Society. He serves as the Editor-in-Chief for the Circuit and Signal Processing Section of the *Electronics* journal (MDPI). He serves as an Area Editor for the *International Journal of Electronics and Communications* (AEUE) journal and an Editor for the *International Journal of Circuit Theory and Applications*. He is an Associate Editor of the *Circuits, Systems, and Signal Processing* journal and the *Journal of Advanced Research*. He is an Editorial Board Member of the *Microelectronics Journal*, *Analog Integrated Circuits and Signal Processing* journal, *IETE Journal of Education*, *Fractal and Fractional* journal, and *Journal of Low Power Electronics and Applications*.

AHMED S. ELWAKIL (Senior Member, IEEE) was born in Cairo, Egypt. He received the B.Sc. and M.Sc. degrees in electronics and communications from Cairo University, Egypt, and the Ph.D. degree in electrical and electronic engineering from the National University of Ireland, University College Dublin. He also held visiting positions with Istanbul Technical University, Turkey; Queens University, Belfast, U.K.; the Technical University of Denmark, Lyngby, Denmark; and the King Abdullah University of Science and Technology, Saudi Arabia. He is currently a Full Professor with the University of Sharjah, United Arab Emirates; the University of Calgary, AB, Canada; and the Nanoelectronics Integrated Systems Center (NISC) Research Center, Nile University, Cairo. His research interests include circuit theory, nonlinear dynamics, chaos theory, and fractional-order circuits and systems with diverse applications ranging from the modeling of oscillatory networks and nonlinear behavior in electronic circuits and plasma physics to modeling of energy storage devices, bio-materials, and biological tissues. He has authored or coauthored more than 350 publications in these areas (current H-index 45). He has been a member of the IEEE Technical Committee on Nonlinear Circuits and Systems, since 2000. He was a recipient of the Egyptian Government First Class Medal for achievements in engineering sciences, in 2015, and the UAE President Award (Khalifa Award), in 2020. He is an International Observer in the European Cooperation in Science and Technology (COST) action on fractional-order system analysis synthesis and their importance for future design (CA15225) and an Expert with the United Nations Development Program (UNDP). He was on the editorial board of the IEEE JOURNAL ON EMERGING AND SELECTED TOPICS IN CIRCUITS AND SYSTEMS and an Associate Editor of the IEEE TRANSACTIONS ON CIRCUITS AND SYSTEMS—I: REGULAR PAPERS. He currently serves as the Editor-in-Chief for the *International Journal of Circuit Theory and Applications* (Wiley) and an Associate Editor for the *International Journal of Electronics and Telecommunications* (AEUE and Elsevier).

DRAZEN JURISIC (Member, IEEE) received the B.Sc., M.Sc., and Ph.D. degrees in electrical engineering from the University of Zagreb, Croatia, in 1990, 1995, and 2002, respectively. From 1997 to 1999, he was with the Institute of Signal and Information Processing, Swiss Federal Institute of Technology (ETH), Zürich, Switzerland. Since 2008, he has been visiting the Faculty of Engineering, Bar-Ilan University, Israel, and doing research in the field of analog circuits and filters. He is currently a Full Professor with the Faculty of Electrical Engineering and Computing (FER), University of Zagreb. He lectures in the field of electrical circuits, signals and systems, and analog and mixed-signal processing circuitry. His research interests include analog and digital signal processing and filter designs, integrated circuit designs, and the study and analysis of fractional-order systems. He has been a MC Member of the COST Action CA15225 "Fractional-Order Systems: Analysis, Synthesis and Their Importance for Future Design." He is a member of the Croatian Society for Communications, Computing, Electronics, Measurement and Control and the IEEE-CAS Society. He was awarded the Silver Plaque Josip Loncar for his Ph.D. thesis and an IEEE Best Paper Finalist Award for a conference paper.